

LETTER TO THE EDITOR



A broadly neutralizing antibody against SARS-CoV-2 Omicron variant infection exhibiting a novel trimer dimer conformation in spike protein binding

© CEMCS, CAS 2022

Cell Research (2022) 32:862–865; <https://doi.org/10.1038/s41422-022-00684-0>

Dear Editor,

The constant evolution of SARS-CoV-2 has resulted in the emergence of circulating variants during the COVID-19 pandemic. Recently, a newly emerged B.1.1.529 (Omicron) variant raised global concern. Compared with the original SARS-CoV-2 strain and other variants of concern (VOCs), the Omicron variant has more than 30 mutations on its spike (S) protein,¹ of which 16 mutations are located in the receptor-binding domain (RBD). These mutations confer significant resistance to neutralizing antibodies elicited by COVID-19 convalescents^{2,3} or individuals who have received mRNA vaccines^{4,5} or inactivated vaccines.⁶ A recent study indicated that most SARS-CoV-2-specific monoclonal antibodies, including FDA-approved antibodies, have lost efficacy against the Omicron variant.⁷ The Omicron variant has become the dominant strain worldwide, making it urgent to update the vaccination strategy or develop new antibodies to catch up with the pandemic.

Here, we report the isolation of a broadly neutralizing monoclonal antibody, named 6M6 (IGHV3-91, IGLV3-21), from an individual who recovered from COVID-19.⁸ 6M6 showed strong binding to both S trimer and RBD domain of SARS-CoV-2, including the Omicron variant (Fig. 1a). The binding affinities of 6M6 to the S trimer and RBD of the Omicron variant were 1.5- or 4-fold lower than to those of wild-type (WT) SARS-CoV-2, respectively (Fig. 1b). 6M6 exhibited 3- to 4-fold higher binding affinity than S309 for the S trimer and RBD of Omicron variant, respectively (KD = 3.16 nM vs 8.91 nM and 2.05 nM vs 8.22 nM, Fig. 1b; Supplementary information, Fig. S1).

We assessed the neutralizing ability of 6M6 using pseudoviruses expressing the S protein of WT and Alpha, Beta, Gamma, Delta, and Omicron variants. A panel of well-known antibodies could not neutralize the Omicron variant, except for S309. The neutralization of 6M6 against the Omicron variant was unchanged compared to that against WT, with an IC₅₀ of 19.9 ng/mL, while S309 was 10 times less potent than 6M6 in neutralizing the Omicron variant (IC₅₀ = 221 ng/mL, Fig. 1c). 6M6 remained effective against Alpha, Beta, and Gamma, but was less potent in neutralizing Delta variant (IC₅₀ = 653 ng/mL, Fig. 1c). 6M6 exhibited similar neutralization pattern against authentic viruses compared to pseudoviruses. It potentially neutralized the authentic WT, Alpha, Beta, and Omicron, except Delta (Fig. 1d).

Competition assays were then performed with bilayer interferometry (BLI) to evaluate the binding site of 6M6. 6M6 competed with S309 for binding to the RBD protein of SARS-CoV-2, suggesting that 6M6 binds to an epitope that overlaps with S309 (Fig. 1e). 6M6 did not compete with ACE2 for binding to the SARS-CoV-2 RBD (Fig. 1f), which is similar with S309, confirming that the epitope of 6M6 does not overlap with the ACE2-binding

site. However, 6M6 prevented the Omicron S trimer from binding to ACE2 (Fig. 1g), while S309 did not affect the ACE2–S trimer interaction. These data suggest that 6M6 binds to the Omicron S trimer in a unique conformation and blocks SARS-CoV-2 virion infection.

To investigate the neutralization mechanism of 6M6, we determined the cryo-EM structure of the prefusion-stabilized SARS-CoV-2 Omicron S ectodomain trimer complexed with 6M6 (Omicron S–6M6). Two states of the complex, trimer and trimer dimer, were determined at resolutions of 3.18 Å and 3.45 Å, respectively (Fig. 1h; Supplementary information, Figs. S2, S3 and Table S1).

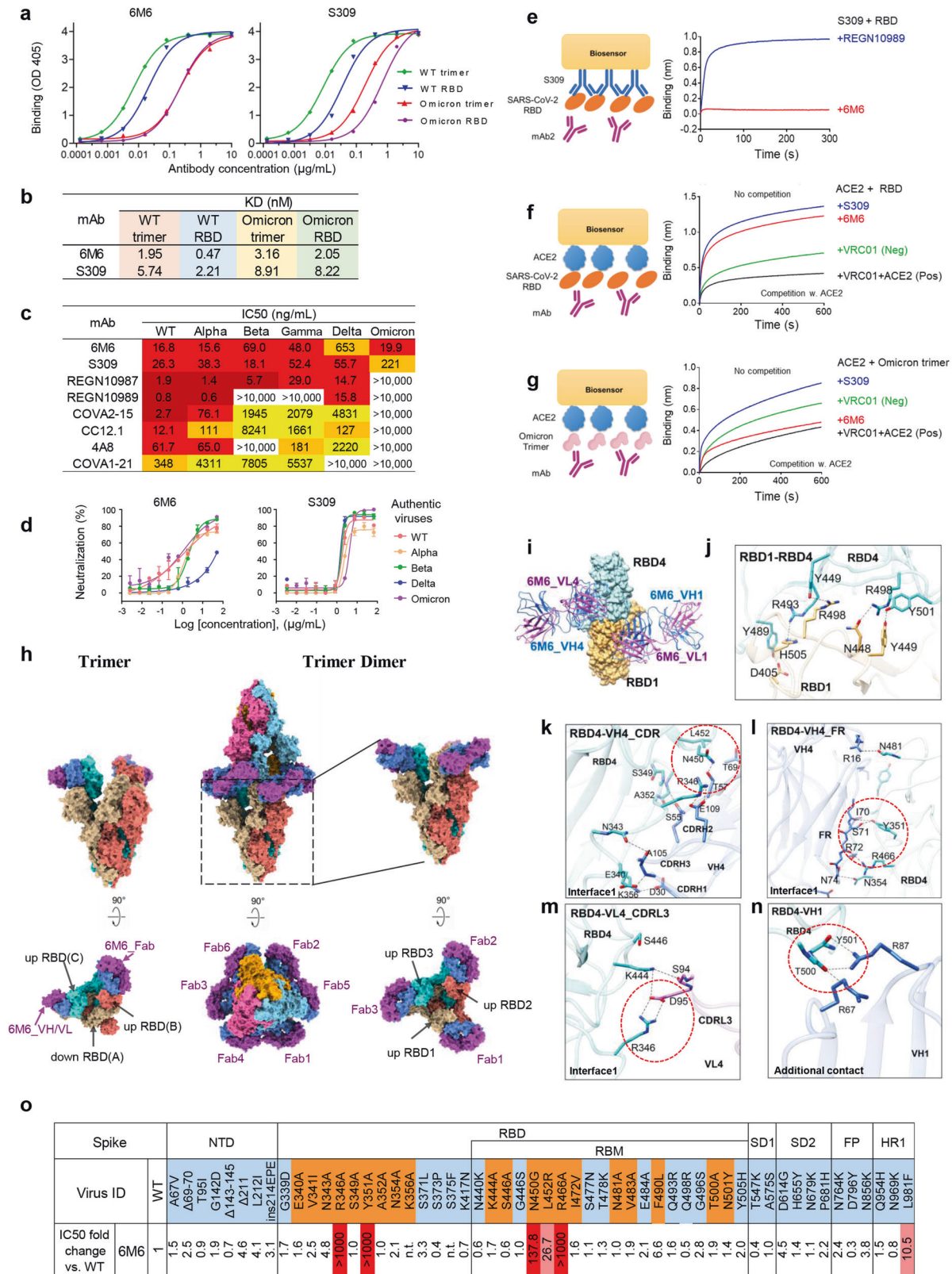
The majority of the S–6M6 particles (~70% particles) are trimers, which include one down-RBD and two up-RBDs, with each up RBD binding with one 6M6 Fab (Fig. 1h). The rest particles (~30%) adopt a special trimer dimer conformation formed by two trimers, in which all six RBDs are in the “up” state and interact with six 6M6 Fabs. In total, three IgGs interact with two S trimers and induce the formation of trimer dimer. The Fc region is missing in the final model because of its flexibility, though weak density is observed in the cryo-EM map (Fig. 1h; Supplementary information, Fig. S4).

In both states, 6M6 Fabs target the same epitopes of RBD, burying the surface area of ~1206 Å². In the trimer dimer state, an additional contact was introduced between 6M6 and the RBD from the other trimer, burying a small surface area of ~229 Å². In trimer dimer, the interaction (interface 1) between RBD4 and the heavy chain (VH4) of 6M6 Fab is primarily due to hydrophilic interactions (Fig. 1i). Intensive hydrogen bonds and salt bridges are formed between CDRs (Fig. 1k) and FR (70-ISRDN-74, R16) (Fig. 1l) on 6M6 VH4 and K356, S349, A352, N450, E340, N343, R346, N354, R466, Y351, and N481 of RBD4. In addition, salt bridges and hydrogen bonds (H-bonds) between CDRL3 of 6M6 VL4 and R346 and K444 from RBD4 further enhanced 6M6 binding (Fig. 1m).

The additional contact in the trimer dimer was formed between RBD and the 6M6 VH region of the other opposite Fab (Fig. 1n). Between RBD4 and 6M6 VH1, this interaction is mainly mediated by H-bonds between R67 and R87 of VH1 and T500 and Y501 of RBD4. Notably, the interaction between RBD1 and 6M6 is slightly different, in which S446 forms an H-bond with S94 of VL1 of 6M6 (Supplementary information, Fig. S5). In addition, the two opposite RBDs also bury an ~575 Å² surface area and form intensive interactions, which are mainly mediated by intensive H-bonds between N448, Y449, D405, R498, and H505 of RBD1 and Y449, Y489, R493, R498, and Y501 of RBD4 (Fig. 1j). Thus, each IgG crosslinks two S trimers by interacting with four RBDs, introducing additional contact between two opposite RBDs, and inducing the formation of a trimer dimer. It has been reported that nanobody

Received: 12 February 2022 Accepted: 9 June 2022

Published online: 29 June 2022



Fu2 interacts simultaneously with two up RBDs from different S trimers of SARS-CoV-2 and induce the formation of trimer dimer.⁹ Similarly, IgG 6M6 simultaneously interacts with two up RBDs from different S trimers and induce the formation of trimer dimer. Explicitly, the negative staining assay showed that only IgG format

but not Fab 6M6 induced S crosslinking (Supplementary information, Fig. S6). Thus, the Fc region of 6M6 is essential to stabilize the trimer dimer. Superimposition of the structure of the 6M6 Fab-Omicron S RBD complex over the ACE2-Omicron S RBD and S309-WT S RBD

Fig. 1 6M6 against SARS-CoV-2 Omicron variant infection with a novel trimer dimer conformation. **a** Binding of 6M6 to the S trimer and RBD of WT SARS-CoV-2 and Omicron measured by ELISA. S309 was used as a control. **b** The binding affinity of 6M6 to the S trimer and RBD of WT and Omicron measured by BLI. **c, d** Neutralization of 6M6 against the pseudotyped (**c**) and the authentic (**d**) SARS-CoV-2 and its VOCs including Omicron. S309 and indicated mAbs were used as controls. **e** Binding of 6M6 to WT RBD in competition with S309 measured by BLI. **f, g** Binding of ACE2 to SARS-CoV-2 RBD (**f**) or Omicron S trimer (**g**) in competition with 6M6 (red), S309 (blue). An HIV-1 antibody VRC01 was used as an IgG1 isotype negative control (green) and the mixture of VRC01 and ACE2 was used as a positive control (black). **h** Cryo-EM structures of the Omicron S trimer in complex with 6M6. 6M6 binds to Omicron S in trimer and trimer dimer states. Two perpendicular views of Omicron S-6M6 depict the surface, with the VH/CH domain in blue and VL/CL in orchid. **i** Close-up view of the interactions between 6M6 and the Omicron RBD. Omicron RBD1 and RBD4 are displayed on the yellow and blue surfaces, respectively. The heavy chain and light chain are shown as cartoons colored blue and magenta, respectively. **j** The interaction between RBD1 and RBD4 in trimer dimer. **k–m** The detailed interactions of 6M6 CDR (**k**), FR (**l**) of VH4, VL4 (**m**) with Omicron RBD4 (interface 1). Residues participating in interactions are represented as sticks. Polar interactions are indicated as dotted lines. The residues involved in different interactions are enclosed in red dotted circles. **n** The additional contact of 6M6 VH1 with Omicron RBD4 (interface 2) in trimer dimer. **o** Neutralization of 6M6 against a panel of 54 SARS-CoV-2 single mutants, including 34 single mutants found within the Omicron variant (highlighted in light blue) and 20 single mutants involved in 6M6 binding (highlighted in orange). Fold change is calculated as the IC_{50} of the mutant/the IC_{50} of WT. Mutants that decreased the sensitivity of 6M6 with fold change values between 10 and 100 are highlighted in pink, and fold change values > 100 are highlighted in red. K356A and S375F pseudoviruses were not available and are labeled as not tested, “n.t.”

complex structures revealed that 6M6 engages an epitope outside the receptor-binding motif (RBM) and does not clash with ACE2 upon binding to S (Supplementary information, Fig. S7), which is consistent with the competition assay (Fig. 1f). The structure of the 6M6 trimer dimer indicates that three IgG molecules cross-link the S-glycoprotein trimer and cause steric hindrance or virion aggregation, which explains the ability of 6M6 to fully neutralize Omicron virions.

To verify the key epitope of 6M6, we analyzed the RBD residues involved in binding 6M6 (Supplementary information, Fig. S7c) and constructed a panel of 54 SARS-CoV-2 single mutants, including 20 RBD single mutants that play major roles in binding 6M6 (highlighted in orange, Fig. 1o) as well as 34 mutants found in Omicron (highlighted in light blue, Fig. 1o). S371L mutation was reported to resist most of the NAbs.¹⁰ The control antibody S309 used in this study also showed 28.6-fold decrease in neutralizing activity (data not shown). However, S371L was sensitive to 6M6. The L981F mutation from Omicron decreased the neutralizing activities of 6M6 by 10.5-fold. However, when L981F and 33 other mutations were combined in Omicron, they did not confer resistance to 6M6 at all. Residues R346, Y351, N450, and R466 form H-bonds with 6M6 (Fig. 1k–m; Supplementary information, Fig. S5). Mutations of R346A, Y351A, N450G, and R466A greatly decreased the neutralizing activities of 6M6 (>100-fold, Fig. 1o). Structural analysis showed that residue L452 forms electrostatic interaction with T69 of 6M6 VH (Fig. 1k). Decreased neutralizing activities of 6M6 to the L452R mutation, by 26.7-fold (Fig. 1o), explained the reduced neutralizing activity of 6M6 on Delta variant (Fig. 1c, d) since Delta includes L452R mutation. The L452R mutation may disturb the interaction between RBD and Fab because of the longer chain of Arg. Therefore, residues R346, Y351, N450, L452, and R466 are critical residues between the interactions of RBD and 6M6.

We compared the broadly neutralizing antibodies against all the six tested VOCs. These antibodies can be classified into three categories according to the epitope location on RBD (Supplementary information, Fig. S8).

Taken together, the potency and breadth of antibody 6M6 suggest it as a potential candidate therapeutic drug against Omicron. The trimer dimer structure of Omicron S-6M6, in which all six “up” RBDs interacted with six 6M6 Fabs, revealed a novel and excellent neutralization mechanism of 6M6, through which 6M6 fully neutralized Omicron by steric hindrance or virion aggregation.

Yingdan Wang^{1,5}, Wuqiang Zhan^{1,5}, Jianguan Liu^{1,2,5}, Yanqun Wang^{3,5}, Xiang Zhang¹, Meng Zhang¹, Lin Han¹, Yunping Ma¹, Lu Lu¹, Yumei Wen¹, Zhenguo Chen¹, Jincun Zhao^{3,4}, Fan Wu², Lei Sun¹ and Jinghe Huang¹

¹Key Laboratory of Medical Molecular Virology (MOE/NHC/CAMS) and Shanghai Institute of Infectious Disease and Biosecurity, Shanghai Fifth People's Hospital, Shanghai Public Health Clinical Center, Institutes of Biomedical Sciences, School of Basic Medical Sciences, Fudan University, Shanghai, China. ²Shanghai Immune Therapy Institute, Shanghai Jiao Tong University School of Medicine Affiliated Renji Hospital, Shanghai, China. ³State Key Laboratory of Respiratory Disease, National Clinical Research Center for Respiratory Disease, Guangzhou Institute of Respiratory Health, the First Affiliated Hospital of Guangzhou Medical University, Guangzhou, Guangdong, China. ⁴Institute of Infectious Disease, Guangzhou Eighth People's Hospital of Guangzhou Medical University, Guangzhou, Guangdong, China. ⁵These authors contributed equally: Yingdan Wang, Wuqiang Zhan, Jianguan Liu, Yanqun Wang. ✉email: zhaojincun@gird.cn; wufan@fudan.edu.cn; llsun@fudan.edu.cn; Jinghehuang@fudan.edu.cn

DATA AVAILABILITY

The cryo-EM map and the coordinates of SARS-CoV-2 Omicron S complexed with 6M6 have been deposited to the Electron Microscopy Data Bank (EMDB) and Protein Data Bank (PDB) with accession numbers EMD-32552 and PDB 7WJY (trimer), EMD-32553 and PDB 7WJZ (trimer dimer), EMD-32554 and PDB 7WK0 (NTD-RBD-6M6 local refinement).

REFERENCES

- WHO. [https://www.who.int/news/item/26-11-2021-classification-of-omicron-\(b.1.1.529\)-sars-cov-2-variant-of-concern](https://www.who.int/news/item/26-11-2021-classification-of-omicron-(b.1.1.529)-sars-cov-2-variant-of-concern) (2021).
- Wang, Y. et al. *Emerg. Microbes Infect.* **11**, 424–427 (2022).
- Carreño, J. M. et al. *Nature* **602**, 682–688 (2022).
- Cele, S. et al. *Nature* **602**, 654–656 (2022).
- Schmidt, F. et al. *N. Engl. J. Med.* **386**, 599–601 (2022).
- Ai, J. et al. *Emerg. Microbes Infect.* **11**, 337–343 (2022).
- Cao, Y. et al. *Nature* **602**, 657–663 (2022).
- Wu, F. et al. *JAMA Int. Med.* **180**, 1356–1362 (2020).
- Hanke, L. et al. *Nat. Commun.* **13**, 155 (2022).
- Liu, L. et al. *Nature* **602**, 676–681 (2022).

ACKNOWLEDGEMENTS

This work was supported by the Shanghai Municipal Science and Technology Major Project (ZD2021CY001), National Natural Science Foundation of China (31771008 to J.H.), the Ministry of Science and Technology of China (2021YFC2302500 to L.S.), the National Science and Technology Major Projects of China (2017ZX10202102 to J.H. and 2018ZX10301403 to F.W.), the Shanghai Municipal Commission of Health and Family Planning (2018BR08 to J.H.), the Chinese Academy of Medical Sciences (2019PT350002 to J.H.), and the Talent Development Plan funded by Shanghai Fifth People's Hospital, Fudan University (2020WYRCSG10 to L.H.).

AUTHOR CONTRIBUTIONS

J.H., L.S., and F.W. conceived and designed the experiments. J.H. and F.W. performed B cell sorting and antibody cloning. Y.D.W., J.L., Y.M., and L.L. constructed SARS-CoV-2 pseudovirus mutants, performed neutralization assay, ELISA, and bilayer interferometry experiments. L.S., W.Z., X.Z., Z.C., M.Z., and L.H. performed the structural studies. J.Z. and Y.Q.W. performed authentic virus experiments. Y.W. supervised the project. J.H., Y.D.W., Y.M., L.S., W.Z., X.Z., and Y.Q.W. analyzed the data. J.H., L.S., and F.W. wrote the manuscript.

COMPETING INTERESTS

Patents about the 6M6 in this study are pending.

ADDITIONAL INFORMATION

Supplementary information The online version contains supplementary material available at <https://doi.org/10.1038/s41422-022-00684-0>.

Correspondence and requests for materials should be addressed to Jincun Zhao, Fan Wu, Lei Sun or Jinghe Huang.

Reprints and permission information is available at <http://www.nature.com/reprints>